

A Message Passing based Adaptive PDA Algorithm for Robust Radio-based Localization and Tracking

Alexander Venus^{1,2}, Erik Leitinger¹, Stefan Tertinek³, and Klaus Witrisal^{1,2}

¹Graz University of Technology, Austria, ³NXP Semiconductors, Austria,

²Christian Doppler Laboratory for Location-aware Electronic Systems

Abstract—We present a message passing algorithm for localization and tracking in multipath-prone environments that implicitly considers obstructed line-of-sight situations. The proposed adaptive probabilistic data association algorithm infers the position of a mobile agent using multiple anchors by utilizing delay and amplitude of the multipath components (MPCs) as well as their respective uncertainties. By employing a non-uniform clutter model, we enable the algorithm to facilitate the position information contained in the MPCs to support the estimation of the agent position without exact knowledge about the environment geometry. Our algorithm adapts in an online manner to both, the time-varying signal-to-noise-ratio and line-of-sight (LOS) existence probability of each anchor. In a numerical analysis we show that the algorithm is able to operate reliably in environments characterized by strong multipath propagation, even if a temporary obstruction of all anchors occurs simultaneously.

Index Terms—Obstructed Line-Of-Sight, Multipath, Message Passing, Probabilistic Data Association, Belief Propagation

I. INTRODUCTION

Radio-based localization in environments such as indoor or urban territories is still a challenging task [1], [2]. These environments are characterized by strong multipath propagation and frequent obstructed line-of-sight (OLOS) situations, which can prevent the correct extraction of the line-of-sight (LOS) component (see Fig. 1). For safety and security critical applications, such as keyless entry systems [3] or autonomous driving [4], robustness, i.e., a low probability of localization outage, is of critical importance.

Therefore, new systems take advantage of multipath channels by estimating multipath components (MPCs) for localization [5], [6], exploiting cooperation among agents [7], or signal processing against multipath propagation and clutter measurements, i.e., outliers, in general [8]–[10].

The probabilistic data association filter [11] is a Gaussian variant of probabilistic data association (PDA), which is able to incorporate multiple anchors (sensors) [11] and amplitude information (AI-PDAF [12]), but suffers from being computationally intractable or its dependence on mode-matching.

This paper proposes a low-complexity message passing based multi-sensor PDA algorithm that estimates and tracks the state of a mobile agent by utilizing delay and amplitude of multipath components (MPCs) as well as their respective

The financial support by the Christian Doppler Research Association, the Austrian Federal Ministry for Digital and Economic Affairs and the National Foundation for Research, Technology and Development is gratefully acknowledged.

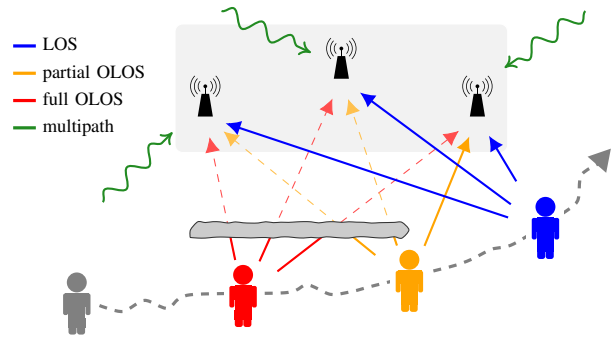


Fig. 1. The mobile agent is walking alongside the anchors on an example trajectory. Due to an obstacle, the LOS to all anchors is not always available. There occur partial, as well as full OLOS situations.

uncertainties. The proposed algorithm adapts in an online manner to both, the time-varying signal-to-noise-ratio (SNR) [5] and LOS existence probability of each anchor [13]. Furthermore, we use a non-uniform non-LOS (NLOS) model, which comprises measurements originating from MPCs, as well as false alarms (FAs), which do not have a physical explanation (similar to [14]). This model enables the algorithm to utilize the position information contained in the MPCs in order to support the estimation of the agent state without specific map information and, hence, to operate reliably in environments with strong multipath propagation and temporary obstructed LOS situations. In that sense, the proposed algorithm allows to indirectly exploit MPCs. The key contributions of this paper are as follows.

- We present a multi-sensor message passing algorithm with combined SNR and LOS existence probability tracking.
- We employ a non-uniform NLOS probability density function (PDF) using a double-exponential model for the multipath likelihood function (LHF).
- We show the applicability of our algorithm in the context of OLOS mitigation and evaluate the influence of the features of our algorithm in a numerical analysis.

Note that for this work it is assumed that the parameters of the NLOS object are known constants. This shortcoming shall be addressed in an extended version of this work, and is further discussed in Section VII.

II. SIGNAL MODEL

At each discrete time $n \in \{1, \dots, N\}$, the mobile agent at position \mathbf{p}_n transmits a signal $s(t)$ and each anchor $j \in$

$\{1, \dots, J\}$ at anchor position $\mathbf{p}_A^{(j)} = [p_{Ax}^{(j)} \ p_{Ay}^{(j)}]^T$ acts as a receiver. The complex baseband signal received at the j th anchor is modeled as

$$r_n^{(j)}(t) = \alpha_{n,0}^{(j)} s(t - \tau_{n,0}^{(j)}) + \sum_{k=1}^{K_n^{(j)}} \alpha_{n,k}^{(j)} s(t - \tau_{n,k}^{(j)}) + w_n^{(j)}(t) \quad (1)$$

The first and second term describe the LOS component and the sum of $K_n^{(j)}$ specular MPCs with their corresponding complex amplitudes $\alpha_{n,k}^{(j)}$ and delays $\tau_{n,k}^{(j)}$, respectively. The third term $w_n^{(j)}(t)$ is additive white Gaussian noise with double-sided power spectral density $N_0/2$. The MPCs arise from reflection or scattering by unknown objects, since we assume that no map information is available as indicated in Fig. 1 by green lines.

III. CHANNEL ESTIMATION

The received signal (1) is sampled and, by applying a suitable snapshot based channel estimation and detection algorithm [15], [16], one obtains at each time n and anchor j , a number of $M_n^{(j)}$ measurements denoted by $\mathbf{z}_{n,m}^{(j)}$, with measurement indices $m \in \mathcal{M}_n^{(j)} = \{1, \dots, M_n^{(j)}\}$. Each $\mathbf{z}_{n,m}^{(j)} = [\hat{d}_{n,m}^{(j)} \ \hat{u}_{n,m}^{(j)} \ \hat{\sigma}_{dn,m}^{(j)}]^T$ contains a distance measurement $\hat{d}_{n,m}^{(j)} = c \hat{\tau}_{n,m}^{(j)}$, a normalized signal amplitude measurement $\hat{u}_{n,m}^{(j)} = |\hat{\alpha}_{n,m}^{(j)}| / \hat{\sigma}_{\alpha n,m}^{(j)}$ corresponding to the square root of the SNR, and a distance standard deviation measurement $\hat{\sigma}_{dn,m}^{(j)}$, where $\hat{\tau}_{n,m}^{(j)}$ and $\hat{\alpha}_{n,m}^{(j)}$ represent the corresponding delay and complex amplitude and c is the speed-of-light. If not implicitly provided by the channel estimator, we can obtain $\hat{\sigma}_{dn,m}^{(j)}$ by means $\hat{u}_{n,m}^{(j)}$ using $\hat{\sigma}_{dn,m}^{(j)} = (c \sqrt{8} \pi \beta \hat{u}_{n,m}^{(j)})^{-1}$, with β being the effective bandwidth. This equation corresponds to the Cramér-Rao lower bound (CRLB) for a single-distance measurement [1] and is used for the simulations in Sec. VI. Consider that assuming the statistical model to be correct, the distance variance will attain the CRLB for a single-distance measurement, as the NLOS measurements are taken into account by the data association algorithm.

We define the nested vectors $\mathbf{z}_n^{(j)} = [\mathbf{z}_{n,1}^{(j)T} \dots \mathbf{z}_{n,M_n^{(j)}}^{(j)T}]^T$ and $\mathbf{z}_n = [\mathbf{z}_n^{(1)T} \dots \mathbf{z}_n^{(J)T}]^T$, where the latter denotes the joint measurement vector per time n . All of its components are used as noisy “measurements” by the proposed algorithm.

IV. SYSTEM MODEL

We consider a mobile agent to be moving along an unknown trajectory as depicted in Fig. 1. The current state of the agent is described by the state vector $\mathbf{x}_n = [\mathbf{p}_n^T \ \mathbf{v}_n^T]^T$, which is composed of the mobile agent’s position $\mathbf{p}_n = [p_{xn} \ p_{yn}]^T$ and velocity $\mathbf{v}_n = [v_{xn} \ v_{yn}]^T$. The state evolves over time n according to a predefined state transition PDF $\Upsilon(\mathbf{x}_n | \mathbf{x}_{n-1})$, where the usual first-order Markov assumption is applied [17].

A. Data Association Model

At each time n and for each anchor j , the measurements, i.e., the components of $\mathbf{z}_n^{(j)}$ are subject to data association uncertainty. Thus, it is not known which measurement $\mathbf{z}_{n,m}^{(j)}$ originated from the LOS, or which one is due to an MPC. It is also possible that a measurement $\mathbf{z}_{n,m}^{(j)}$ did not originate

from any physical component, but from FAs of the prior channel estimation and detection algorithm. Our model only distinguishes between “LOS measurements” originating from the LOS and “NLOS measurements”, i.e., measurements due to MPCs or FAs. Based on the concept of PDA [11], we define an association variable

$$a_n^{(j)} = \begin{cases} m \in \mathcal{M}_n^{(j)}, & \mathbf{z}_{n,m}^{(j)} \text{ is the LOS measurement in } \mathbf{z}_n^{(j)} \\ 0, & \text{there is no LOS measurement in } \mathbf{z}_n^{(j)} \end{cases} \quad (2)$$

Assuming the number of NLOS measurements to follow a uniform distribution (so called “non-parametric model”), the joint probability mass function (PMF) of $a_n^{(j)}$ and $M_n^{(j)}$ can be shown to be proportional to the function [11]

$$h(a_n^{(j)}, M_n^{(j)}; u_n^{(j)}, q_n^{(j)}) = \begin{cases} \frac{p_{En}^{(j)}(u_n^{(j)}, q_n^{(j)})}{M_n^{(j)}}, & a_n^{(j)} \in \mathcal{M}_n^{(j)} \\ 1 - p_{En}^{(j)}(u_n^{(j)}, q_n^{(j)}), & a_n^{(j)} = 0 \end{cases} \quad (3)$$

where $p_{En}^{(j)}(u_n^{(j)}, q_n^{(j)})$ is the probability that there is a LOS measurement for the current set of measurements defined in Sec. IV-D and $u_n^{(j)}$ and $q_n^{(j)}$ are defined in Sections IV-C and IV-D, respectively. We also define the joint vectors $\mathbf{a}_n = [a_n^{(1)} \dots a_n^{(J)}]^T$ and $\mathbf{M}_n = [M_n^{(1)} \dots M_n^{(J)}]^T$.

B. Delay/Distance Model

To incorporate the data association procedure into the measurement process we define two LHF, one for the LOS event and one for the NLOS event.

Let the range-only measurement vector be $\tilde{\mathbf{z}}_{n,m}^{(j)} = [\hat{d}_{n,m}^{(j)} \ \hat{\sigma}_{dn,m}^{(j)}]^T$. First we define the LOS LHF as

$$f_L(\tilde{\mathbf{z}}_{n,m}^{(j)} | \mathbf{p}_n) = \mathcal{N}(\hat{d}_{n,m}^{(j)}; d_{\text{LOS}n}^{(j)}(\mathbf{p}_n), \hat{\sigma}_{dn,m}^{(j)}) \quad (4)$$

where $\mathcal{N}(\cdot)$ denotes a Gaussian PDF of the random variable (RV) $\hat{d}_{n,m}^{(j)}$ with mean $d_{\text{LOS}n}^{(j)}(\mathbf{p}_n)$ and standard deviation $\hat{\sigma}_{dn,m}^{(j)}$. The LOS distance is geometrically related to the agent position via

$$d_{\text{LOS}n}^{(j)}(\mathbf{p}_n) = \|\mathbf{p}_n - \mathbf{p}_A^{(j)}\|. \quad (5)$$

Next, we define the NLOS LHF as [14]

$$f_{\text{NL}}(\tilde{\mathbf{z}}_{n,m}^{(j)} | \mathbf{p}_n) = P_{\text{MP}} f_{\text{MP}}(\hat{d}_{n,m}^{(j)} | \mathbf{p}_n) + (1 - P_{\text{MP}}) f_{\text{FA}}(\hat{d}_{n,m}^{(j)}), \quad (6)$$

which represents a weighted sum of two LHF, with P_{MP} acting as a weighting coefficient: The FA LHF $f_{\text{FA}}(\hat{d}_{n,m}^{(j)}) = \mathcal{U}(0, d_{\text{max}})$, which is a uniform distribution with the maximum distance d_{max} and the multipath LHF

$$f_{\text{MP}}(\hat{d}_{n,m}^{(j)} | \mathbf{p}_n) = \begin{cases} \frac{\gamma_f + \gamma_r}{\gamma_f^2} (1 - e^{-\frac{\Delta_{n,m}^{(j)}}{\gamma_f}}) e^{-\frac{\Delta_{n,m}^{(j)}}{\gamma_r}}, & \Delta_{n,m}^{(j)} > 0 \\ 0, & \Delta_{n,m}^{(j)} \leq 0 \end{cases} \quad (7)$$

which is a double exponential function [18] with the distance difference $\Delta_{n,m}^{(j)} = \hat{d}_{n,m}^{(j)} - d_{\text{LOS}n}^{(j)}(\mathbf{p}_n) - B$. γ_r is the rise distance, γ_f the fall distance, and B is a bias value.

Finally, we define the overall-distance LHF as

$$f(\tilde{\mathbf{z}}_{n,m}^{(j)} | \mathbf{p}_n, a_n^{(j)}) = \begin{cases} f_L(\tilde{\mathbf{z}}_{n,m}^{(j)} | \mathbf{p}_n), & a_n^{(j)} = m \\ f_{\text{NL}}(\tilde{\mathbf{z}}_{n,m}^{(j)} | \mathbf{p}_n), & a_n^{(j)} \neq m \end{cases} \quad (8)$$

The shape of (8) is depicted in Fig. 2a.

C. Amplitude Model

As for the delay model in Sec. IV-B, we start by defining the LOS amplitude LHF as $f_L(\hat{u}_{n,m}^{(j)}|u_n^{(j)}) \propto f_{\text{Rice}}(\hat{u}_{n,m}^{(j)}; 1, u_n^{(j)}) \nu(\hat{u}_{n,m}^{(j)} - \gamma)$ and the NLOS amplitude LHF as $f_{\text{NL}}(\hat{u}_{n,m}^{(j)}) \propto f_{\text{Rayl}}(\hat{u}_{n,m}^{(j)}; 1) \nu(\hat{u}_{n,m}^{(j)} - \gamma)$, where $\nu(\hat{u}_{n,m}^{(j)} - \gamma)$ is the unit step function with threshold γ that truncates the distributions. The PDF f_{Rice} is a Rician distribution and PDF f_{Rayl} is a Rayleigh distribution with non-centrality parameter $u_n^{(j)}$ and respective spread parameters equal to 1. Note that due to truncation the functions need to be scaled to represent proper PDFs [12]. The overall-amplitude LHF is given by

$$f(\hat{u}_{n,m}^{(j)}|u_n^{(j)}, a_n^{(j)}) = \begin{cases} f_L(\hat{u}_{n,m}^{(j)}|u_n^{(j)}), & a_n^{(j)} = m \\ f_{\text{NL}}(\hat{u}_{n,m}^{(j)}), & a_n^{(j)} \neq m \end{cases} \quad (9)$$

which is shown in Fig. 2b. This model represents the distribution of amplitude estimates of a single complex baseband signal in additive Gaussian noise obtained using maximum likelihood estimation and generalized likelihood ratio test detection [19]–[21]. Consider that for the model to be true, the MPCs in (1), i.e., all components except for the LOS, have to be represented by a stochastic process with zero mean (i.e. dense multipath component model [1]). The above definition is similar to [12]. However, we use the normalized amplitude $u_n^{(j)}$ [22], i.e., the spreading parameters of the Rayleigh and Rician distribution, which constitute the overall-amplitude LHF (9), are equal to 1, avoiding the necessity to track these parameters. We model the temporal evolution of $u_n^{(j)}$ as a first order Markov process, which is defined by a state transition PDF $\Phi(u_n^{(j)}|u_{n-1}^{(j)})$. The amplitudes of all anchors j are assumed to be independent stochastic processes, ignoring possible geometric information available, as for channels with strong multipath propagation received signal strength measurements tend to be error prone. We also define the joint amplitude vector $\mathbf{u}_n = [u_n^{(1)} \dots u_n^{(J)}]^T$.

D. LOS Existence Probability Model

We model the LOS existence probability given in (3) as $p_{\text{En}}^{(j)}(u_n^{(j)}, q_n^{(j)}) = p_{\text{Dn}}^{(j)}(u_n^{(j)}) q_n^{(j)}$. The so-called probability of detection $p_{\text{Dn}}^{(j)}(u_n^{(j)})$ is modelled according to Sec. IV-C by assuming that the proposed algorithm is applied after a generalized likelihood ratio test detector. That is, $p_{\text{Dn}}^{(j)}(u_n^{(j)})$ is completely determined by the normalized amplitude $u_n^{(j)}$ and γ , which represents the detection threshold and is a constant to be chosen. $q_n^{(j)}$ is the probability of the event that the LOS is *not* obstructed, which is referred to as LOS probability in the following, and acts as a prior probability to the detection event. According to [13], [23], we model $q_n^{(j)}$ as discrete RV that takes its values from a finite set $\mathcal{Q} = \{\omega_1, \dots, \omega_Q\}$, where $\omega_i \in (0, 1]$. The temporal evolution of $q_n^{(j)}$ is modelled by a first-order Markov process, which results in a conventional Markov chain, with $[\mathbf{Q}^{(j)}]_{i,k} = \Psi(q_n^{(j)} = \omega_i | q_{n-1}^{(j)} = \omega_k)$ being the elements of the transition matrix. The LOS probabilities

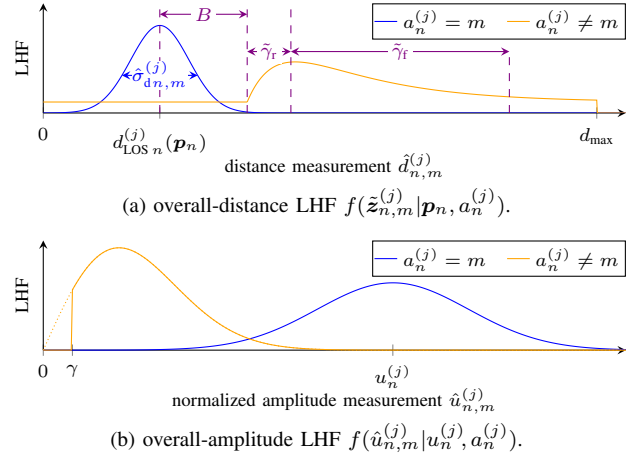


Fig. 2. Graphical representation of the stochastic models constituting the overall LHF for a single measurement.

for different sensors j are assumed to be independent. We also define the joint LOS probability vector $\mathbf{q}_n = [q_n^{(1)} \dots q_n^{(J)}]^T$.

E. Joint Measurement Likelihood Function

Under commonly used assumptions about the statistics of the measurements [24], the joint LHF for all measurements per anchor j and time n can be written as

$$f(\mathbf{z}_n^{(j)}|\mathbf{p}_n, u_n^{(j)}, a_n^{(j)}) = \prod_{m=1}^{M_n^{(j)}} f(\tilde{\mathbf{z}}_{n,m}^{(j)}|\mathbf{p}_n, a_n^{(j)}) f(\hat{u}_{n,m}^{(j)}|u_n^{(j)}, a_n^{(j)}) \quad (10)$$

By neglecting all constant terms, we define the pseudo LHF

$$\begin{aligned} g(\mathbf{z}_n^{(j)}; \mathbf{p}_n, u_n^{(j)}, a_n^{(j)}) &= \prod_{m=1}^{M_n^{(j)}} f_{\text{NL}}(\tilde{d}_{n,m}^{(j)}|\mathbf{p}_n) \times \begin{cases} 1, & a_n^{(j)} = 0 \\ \Lambda(\mathbf{z}_{n,a_n^{(j)}}^{(j)}|\mathbf{p}_n, u_n^{(j)}), & a_n^{(j)} \in \mathcal{M}^{(j)} \end{cases} \end{aligned} \quad (11)$$

where

$$\Lambda(\mathbf{z}_{n,a_n^{(j)}}^{(j)}|\mathbf{p}_n, u_n^{(j)}) = \frac{f_L(\tilde{\mathbf{z}}_{n,a_n^{(j)}}^{(j)}|\mathbf{p}_n) f_L(\hat{u}_{n,a_n^{(j)}}^{(j)}|u_n^{(j)})}{f_{\text{NL}}(\tilde{\mathbf{z}}_{n,a_n^{(j)}}^{(j)}|\mathbf{p}_n) f_{\text{NL}}(\hat{u}_{n,a_n^{(j)}}^{(j)})} \quad (12)$$

is the likelihood ratio. Note that the product of all NLOS events in (11) is not a constant and thus cannot be neglected.

F. Joint Posterior and Factor Graph

Let $\mathbf{z} = [\mathbf{z}_1^T \dots \mathbf{z}_n^T]^T$, $\mathbf{x} = [\mathbf{x}_1^T \dots \mathbf{x}_n^T]^T$, $\mathbf{a} = [\mathbf{a}_1^T \dots \mathbf{a}_n^T]^T$, $\mathbf{u} = [\mathbf{u}_1^T \dots \mathbf{u}_n^T]^T$, $\mathbf{q} = [\mathbf{q}_1^T \dots \mathbf{q}_n^T]^T$, and $\mathbf{M} = [\mathbf{M}_1^T \dots \mathbf{M}_n^T]^T$. Applying Bayes' rule as well as some commonly used independence assumptions [9], [24] the joint posterior for all states up to time n and all J anchors, can be derived up to a constant factor as

$$\begin{aligned} &f(\mathbf{x}, \mathbf{a}, \mathbf{u}, \mathbf{q}, \mathbf{M}|\mathbf{z}) \\ &\propto f(\mathbf{z}|\mathbf{x}, \mathbf{a}, \mathbf{u}, \mathbf{q}) f(\mathbf{x}, \mathbf{a}, \mathbf{u}, \mathbf{q}) \\ &= f(\mathbf{z}|\mathbf{x}, \mathbf{a}, \mathbf{u}, \mathbf{q}) f(\mathbf{a}|\mathbf{u}, \mathbf{q}) f(\mathbf{x}) p(\mathbf{q}) f(\mathbf{u}) \\ &\propto f(\mathbf{x}_0) \prod_{j=1}^J p(q_0^{(j)}) f(u_0^{(j)}) \prod_{n'=1}^n \Upsilon(\mathbf{x}_{n'}|\mathbf{x}_{n'-1}) \Phi(u_{n'}^{(j)}|u_{n'-1}^{(j)}) \\ &\quad \times \Psi(q_{n'}^{(j)}|q_{n'-1}^{(j)}) \tilde{g}(\mathbf{z}_{n'}^{(j)}; \mathbf{p}_{n'}, u_{n'}^{(j)}, a_{n'}^{(j)}, q_{n'}^{(j)}), \end{aligned} \quad (13)$$

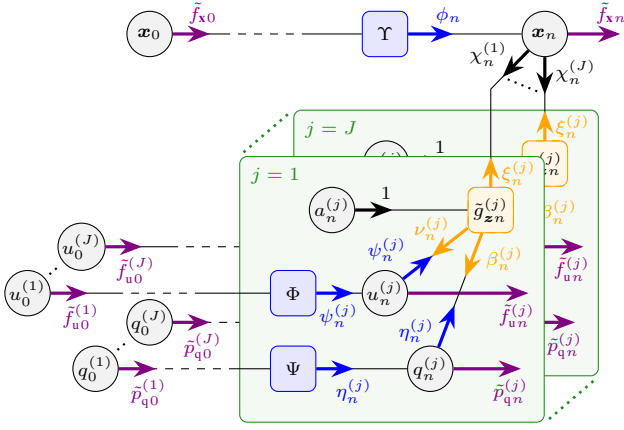


Fig. 3. Factor graph representing the factorization of the joint posterior PDF in (13) and the messages according to the SPA (see Sec. V-B).

with $\tilde{g}(\mathbf{z}_n^{(j)}; \mathbf{p}_n, u_n^{(j)}, a_n^{(j)}, q_n^{(j)}) = h(a_n^{(j)}; \mathbf{x}_n^{(j)}, u_n^{(j)}, q_n^{(j)}) g(\mathbf{z}_n^{(j)}; \mathbf{p}_n, u_n^{(j)}, a_n^{(j)})$. For the sake of brevity, we refer to this expression as $\tilde{g}_{\mathbf{z}_n}^{(j)}(\cdot)$ in the rest of the work. Note that \mathbf{M} is fixed and thus constant, as it is defined implicitly by the measurements \mathbf{z} . This factorization of the joint posterior PDF can be visually represented by the factor graph shown in Fig. 3. Further note that (13) is a mixture of discrete PMFs and continuous PDFs.

V. ALGORITHM

A. Problem Statement

Our goal is to estimate the agent state \mathbf{x}_n . This can be done by calculating the minimum mean-square error (MMSE) [20]

$$\hat{\mathbf{x}}_n^{\text{MMSE}} \triangleq \int \mathbf{x}_n f(\mathbf{x}_n | \mathbf{z}) d\mathbf{x}_n. \quad (14)$$

with $\hat{\mathbf{x}}_n^{\text{MMSE}} = [\hat{\mathbf{p}}_n^{\text{MMSE T}} \hat{\mathbf{v}}_n^{\text{MMSE T}}]^T$. Furthermore, we also calculate

$$\hat{u}_n^{(j)\text{MMSE}} \triangleq \int u_n^{(j)} f(u_n^{(j)} | \mathbf{z}) du_n^{(j)}, \quad (15)$$

$$\hat{q}_n^{(j)\text{MMSE}} \triangleq \sum_{\omega_i \in \mathcal{Q}} \omega_i p(q_n^{(j)} = \omega_i | \mathbf{z}). \quad (16)$$

In order to obtain (14), (15), and (16), marginalization of the joint posterior has to be performed. In general this is computationally infeasible [24]. To counteract this problem, we use a sum-product algorithm (SPA) based algorithm introduced in the next section.

B. Marginal Posterior and Sum-Product Algorithm (SPA)

The marginal posterior can be calculated efficiently by passing messages on the factor graph according to the SPA [25]. The presented algorithm is an adaptation of the algorithms presented in [24], [26] to the factor graph shown in Fig. 3. As the filter shall be executable online, we only pass messages forward in time. This makes the factor graph in Fig. 3 an acyclic graph. For acyclic graphs the SPA yields *exact results* for the marginal posterior [25]. At time n , the following calculations are performed for all J anchors: We start by defining the prediction messages, where $\tilde{f}_{\mathbf{x}_{n-1}}(\cdot)$, $\tilde{f}_{u_{n-1}}^{(j)}(\cdot)$ and $\tilde{p}_{q_{n-1}}^{(j)}(\cdot)$ are messages of the previous time $n-1$, as

$$\phi_n(\mathbf{x}_n) = \int \Upsilon(\mathbf{x}_n | \mathbf{x}_{n-1}) \tilde{f}_{\mathbf{x}_{n-1}}(\mathbf{x}_{n-1}) d\mathbf{x}_{n-1}, \quad (17)$$

$$\psi_n^{(j)}(u_n^{(j)}) = \int \Phi(u_n^{(j)} | u_{n-1}^{(j)}) \tilde{f}_{u_{n-1}}^{(j)}(u_{n-1}^{(j)}) du_{n-1}^{(j)}, \quad (18)$$

$$\eta_n^{(j)}(q_n^{(j)}) = \sum_{q_{n-1}^{(j)}=1}^{N_q} \Psi(q_n^{(j)} | q_{n-1}^{(j)}) \tilde{p}_{q_{n-1}}^{(j)}(q_{n-1}^{(j)}). \quad (19)$$

Next, we define the measurement update messages as

$$\xi_n^{(j)}(\mathbf{x}_n) = \int \psi_n^{(j)}(u_n^{(j)}) \sum_{q_n^{(j)}=1}^{N_q} \eta_n^{(j)}(q_n^{(j)}) \sum_{a_n^{(j)}=1}^{M_n^{(j)}} \tilde{g}_{\mathbf{z}_n}^{(j)}(\cdot) du_n^{(j)}, \quad (20)$$

$$\chi_n^{(j)}(\mathbf{x}_n) = \phi_n(\mathbf{x}_n) \prod_{j'=1}^J \xi_n^{(j')}(\mathbf{x}_n) / \xi_n^{(j)}(\mathbf{x}_n), \quad (21)$$

$$\nu_n^{(j)}(u_n^{(j)}) = \sum_{q_n^{(j)}=1}^{N_q} \eta_n^{(j)}(q_n^{(j)}) \int \chi_n^{(j)}(\mathbf{x}_n) \sum_{a_n^{(j)}=1}^{M_n^{(j)}} \tilde{g}_{\mathbf{z}_n}^{(j)}(\cdot) d\mathbf{x}_n, \quad (22)$$

$$\beta_n^{(j)}(q_n^{(j)}) = \iint \psi_n^{(j)}(u_n^{(j)}) \chi_n^{(j)}(\mathbf{x}_n) \sum_{a_n^{(j)}=1}^{M_n^{(j)}} \tilde{g}_{\mathbf{z}_n}^{(j)}(\cdot) d\mathbf{x}_n du_n^{(j)}. \quad (23)$$

Finally, we calculate the posterior distributions as $f(\mathbf{x}_n | \mathbf{z}) \propto \tilde{f}_{\mathbf{x}_n}(\mathbf{x}_n) = \phi_n(\mathbf{x}_n) \prod_{j=1}^J \xi_n^{(j)}(\mathbf{x}_n)$, $f(u_n^{(j)} | \mathbf{z}) \propto \tilde{f}_{u_n}^{(j)}(u_n^{(j)}) = \psi_n^{(j)}(u_n^{(j)}) \nu_n^{(j)}(u_n^{(j)})$ and $p(q_n^{(j)} | \mathbf{z}) \propto \tilde{p}_{q_n}^{(j)}(q_n^{(j)}) = \eta_n^{(j)}(q_n^{(j)}) \times \beta_n^{(j)}(q_n^{(j)})$. Since a direct calculation of the integrals in equations (17)-(23) is intractable, a particle-based approximation [17] is used. See [26] and [24] for details.

C. Initialization

We propose to initialize the normalized amplitude PDFs as $\tilde{f}_{u_0}^{(j)}(u_0^{(j)}) = \mathcal{U}(0, u_{\max})$, where u_{\max} is a constant to be chosen according to hardware specific limitations. The LOS PMFs are initialized at $q_0^{(j)} = 1$. Regarding the agent state \mathbf{x}_0 , we assume the velocity to be initialized at $\mathbf{v}_0 = \mathbf{0}$, as we do not know in which direction we are moving. Since we cannot make any assumptions about the angle that the agent takes with respect to any of the anchors, it is reasonable to draw the positions \mathbf{p}_0 uniformly on two-dimensional discs around each anchor j , which are bounded by the maximum possible distance d_{\max} and a sample is drawn from each of the J discs with equal probability.

VI. COMPUTATIONAL RESULTS

We evaluate the proposed algorithm using numerical simulation. To investigate the performance independently of the channel estimation and detection algorithm implementation and possible resulting artifacts, we directly generate the measurement vector \mathbf{z} according to the system model in Sec. IV.

A. Simulation Model

In the example scenario investigated, the agent moves along a curvy trajectory from a distant point to the centre of an object where three anchors are mounted (e.g. a car or a door). The trajectory is illustrated in Fig. 4. It is observed

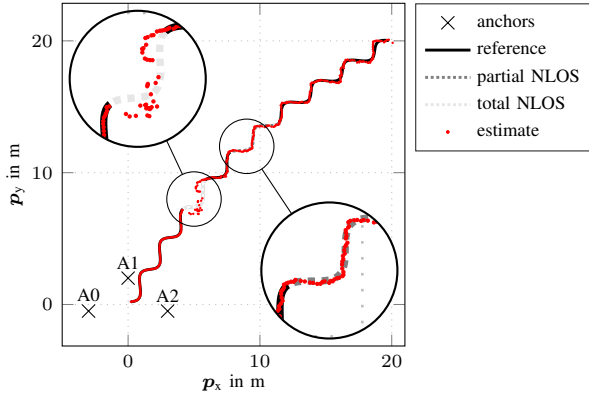


Fig. 4. Simulated trajectory and anchor setup together with a single position estimate, corresponding to the measurement shown in Fig. 5

over a continuous measurement time $t' \in [0, 20]$ s, with a constant sampling rate of $\Delta T = 50$ ms, resulting in $N = 400$ discrete time steps $n \in \{1 \dots N\}$. It comprises two OLOS situations, a partial one, where only the LOS to one anchor is blocked, and a full one, where the LOS to all anchors is blocked. $\|\mathbf{v}_n\|$ is set to vary around a velocity of 1.4 m/s. The normalized amplitudes are set to $\sqrt{30}$ dB at $d_{\text{LOS}n}^{(j)} = 1$ m, with an exponential path-loss factor as low as 0.4 to consider multipath propagation. We used an average rate of 10 NLOS measurements per time n . The parameters of the NLOS LHF, were set to $P_{\text{MP}} = 0.9$, $\gamma_r = 1.5$ m, $\gamma_f = 6$ m, $B = 0.2$ m and $d_{\text{max}} = 50$ m. Fig. 5 shows simulated measurements corresponding to a single realization of the trajectory.

B. Inference Model

In the estimation algorithm, the agent motion, i.e. the state transition PDF $\Upsilon(\mathbf{x}_n | \mathbf{x}_{n-1})$, is modelled by a linear, constant velocity and stochastic acceleration model [27, p. 273], i.e. $\mathbf{x}_n = \mathbf{A} \mathbf{x}_{n-1} + \mathbf{B} \mathbf{w}_n$, with the acceleration process \mathbf{w}_n being i.i.d. across n , zero mean, and Gaussian with covariance matrix $\sigma_a \mathbf{I}$, where \mathbf{I} is a 2x2 identity matrix, $\sigma_a = 0.3$ m/s² is the acceleration standard deviation, and $\mathbf{A} \in \mathbb{R}^{4 \times 4}$ and $\mathbf{B} \in \mathbb{R}^{4 \times 2}$ are defined according to [27, p. 273], with ΔT as defined in Sec. VI-A. The state transition PDF of the normalized amplitudes is modelled as a Gaussian distribution $\Phi(u_n^{(j)} | u_{n-1}^{(j)}) = \mathcal{N}(u_n^{(j)}; u_{n-1}^{(j)}, \sigma_u = 0.2)$, which is independent across n and j . Thus, unlike the simulation model in Sec. VI-A, the amplitudes of all sensors j are assumed to be independent (see Sec. IV-C). We use $\gamma = 0$, which is equivalent to using no detection threshold at all. Thus $p_{\text{D}n}^{(j)}(u_n^{(j)}) = 1$, which leads to $p_{\text{E}n}^{(j)}(u_n^{(j)}, q_n^{(j)}) \equiv q_n^{(j)}$. The set of possible LOS probabilities is chosen as $\mathcal{Q} = \{0.1, 0.2, \dots, 1\}$. The state transition matrix $\mathbf{Q}^{(j)} = \mathbf{Q}$ is set as follows: $[\mathbf{Q}]_{1,1} = 0.9$, $[\mathbf{Q}]_{10,10} = 0.95$, $[\mathbf{Q}]_{2,1} = 0.1$ and $[\mathbf{Q}]_{9,10} = 0.05$. For $2 \leq k \leq 9$, $[\mathbf{Q}]_{k,k} = 0.85$, $[\mathbf{Q}]_{k-1,k} = 0.05$ and $[\mathbf{Q}]_{k+1,k} = 0.1$. For all other tuples $\{i, k\}$, $[\mathbf{Q}]_{i,k} = 0$. We used 10^4 particles for initialization and 10^3 particles for inference during the track.

C. Performance Results

We analyze the influence of the individual features of our algorithm with respect to the scenario described in Sec.

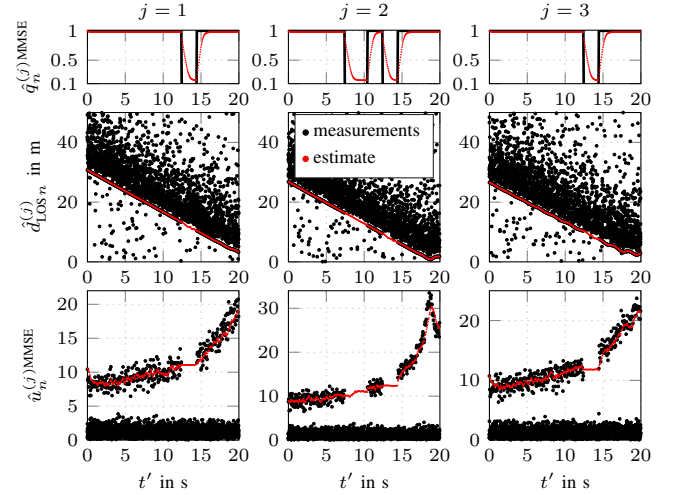


Fig. 5. A single measurement realization and the respective estimates using the proposed algorithm (AL5). $\hat{d}_{\text{LOS}n}^{(j)}$ is calculated using (5) and (14).

VI-A. Fig. 6 shows the algorithm variants implemented and the corresponding features that are enabled for an algorithm (x) or not (). When “ $q_n^{(j)}$ tracking” is deactivated, we set $q_n^{(j)} = 0.999$ for all n, j . When we do not use “CRLB based $\hat{\sigma}_{\text{d}n,m}^{(j)}$ ” measurements (see Sec. III), it is set constant to $\hat{\sigma}_{\text{d}n,m}^{(j)} = 0.1$ m. Not applying the “non-uniform f_{NL} ” means $P_{\text{MP}} = 0$, and deactivating “amplitude information” means $f_{\text{L}}(\hat{u}_{n,m}^{(j)} | u_n^{(j)}) / f_{\text{NL}}(\hat{u}_{n,m}^{(j)}) \triangleq 1$ in (12). All simulation results are shown in terms of the root mean squared error (RMSE) of the estimated agent position $e_n^{\text{RMSE}} = \sqrt{\mathbb{E}[\|\hat{\mathbf{p}}_n^{\text{MMSE}} - \mathbf{p}_n\|^2]}$, evaluated using a numerical simulation with 500 realizations. The RMSE is shown in two ways. First, as a function of the continuous measurement time t' and, second, as the cumulative frequency of the RMSE evaluated over the whole time span ($t' \in [0, 20]$ s), as well as over the time span before the total NLOS situation ($t' \in [0, 14.2]$ s). As a performance benchmark we provide the CRLB for a single position measurement without tracking (SP-CRLB) [28]. Comparing the curves of Fig. 6, one can conclude that the RMSE is significantly lowered when additional features are activated. The RMSE of AL1, which represents a conventional multi-sensor PDA, is constantly above 2 m. This is due to the large percentage of outliers, i.e., realizations where the algorithm completely loses the track. This is slightly improved by tracking $q_n^{(j)}$ (AL2), which leads to a reduced number of lost tracks. For AL3, we activate the amplitude information feature, which, in case of sufficient component SNR, significantly improves the performance as NLOS and LOS measurements can be separated better. AL4 can additionally support the state estimation using NLOS measurements, as (6) depends on the agent position \mathbf{p}_n due to the non-uniform NLOS LHF. This is especially beneficial in the full OLOS situation as it significantly reduces the probability of a lost track. Finally we use CRLB based $\hat{\sigma}_{\text{d}n,m}^{(j)}$ measurements for AL5. This additionally reduces the error, as the variance of the inference model is correctly adjusted to the variance of the channel estimation and detection algorithm.

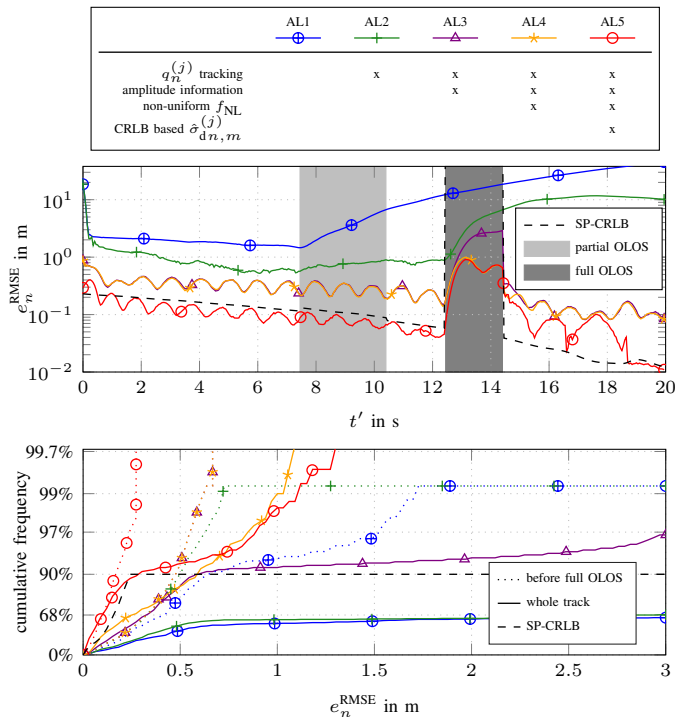


Fig. 6. Performance in terms of the RMSE of the estimated agent position determined using numerical simulation. The upper plot shows the estimated e_n^{RMSE} as a function of the measurement time t' . The lower plot shows the cumulative frequency of the e_n^{RMSE} in inverse logarithmic scale.

VII. CONCLUSION

We have presented a message passing based algorithm that is able to robustly estimate and track the agent's position in multipath channels based on range and amplitude information of multiple sensors as well as their respective uncertainties in both partial and total OLOS situations. We analyzed the performance of the algorithm using numerical simulation and showed that the additional information provided by amplitude information as well as by the NLOS object can support the estimation of the agent state and, thus, reduce the number of lost tracks. In partial OLOS situations the performance of the proposed algorithm attained the CRLB (i.e., no lost tracks).

For this work, we assumed the parameters of the NLOS LHF to be known constants. To overcome this issue, the parameters of the multipath LHF (7) need to be jointly inferred with the agent state. This non-trivial extension requires extended object PDA [29] and shall be addressed in future work.

REFERENCES

- [1] K. Witrisal, P. Meissner *et al.*, "High-accuracy localization for assisted living: 5G systems will turn multipath channels from foe to friend," *IEEE Signal Process. Mag.*, vol. 33, no. 2, pp. 59–70, Mar. 2016.
- [2] A. Shahmansoori, G. E. Garcia *et al.*, "Position and orientation estimation through millimeter-wave MIMO in 5G systems," *IEEE Trans. Wireless Commun.*, vol. 17, no. 3, pp. 1822–1835, Mar. 2018.
- [3] A. Kalyanaraman, Y. Zeng, S. Rakshit, and V. Jain, "CaraoKey : Car states sensing via the ultra-wideband keyless infrastructure," in *Proc. IEEE SECON-20*, 2020, pp. 1–9.
- [4] R. Karlsson and F. Gustafsson, "The future of automotive localization algorithms: Available, reliable, and scalable localization: Anywhere and anytime," *IEEE Signal Process. Mag.*, vol. 34, no. 2, pp. 60–69, 2017.

- [5] E. Leitinger, F. Meyer, F. Hlawatsch, K. Witrisal, F. Tufvesson, and M. Z. Win, "A belief propagation algorithm for multipath-based SLAM," *IEEE Trans. Wireless Commun.*, vol. 18, no. 12, pp. 5613–5629, 2019.
- [6] C. Gentner, T. Jost *et al.*, "Multipath assisted positioning with simultaneous localization and mapping," *IEEE Trans. Wireless Commun.*, vol. 15, no. 9, pp. 6104–6117, Sep. 2016.
- [7] H. Wymeersch, J. Lien, and M. Z. Win, "Cooperative localization in wireless networks," *Proc. IEEE*, vol. 97, no. 2, pp. 427–450, Feb. 2009.
- [8] H. Wymeersch, S. Marano, W. M. Gifford, and M. Z. Win, "A machine learning approach to ranging error mitigation for UWB localization," *IEEE Trans. Wireless Commun.*, vol. 60, no. 6, pp. 1719–1728, 2012.
- [9] E. Leitinger, F. Meyer, P. Meissner, K. Witrisal, and F. Hlawatsch, "Belief propagation based joint probabilistic data association for multipath-assisted indoor navigation and tracking," in *Proc. ICL-GNSS-16*, Barcelona, Spain, June 2016, pp. 1–6.
- [10] F. Meyer, Z. Liu, and M. Z. Win, "Network localization and navigation using measurements with uncertain origin," in *Proc. FUSION-18*, July 2018, pp. 1–7.
- [11] Y. Bar-Shalom and X.-R. Li, *Multitarget-Multisensor Tracking: Principles and Techniques*. Storrs, CT, USA: Yaakov Bar-Shalom, 1995.
- [12] D. Lerro and Y. Bar-Shalom, "Automated tracking with target amplitude information," in *1990 American Control Conference*, May 1990, pp. 2875–2880.
- [13] G. Soldi, F. Meyer, P. Braca, and F. Hlawatsch, "Self-tuning algorithms for multisensor-multitarget tracking using belief propagation," *IEEE Trans. Signal Process.*, vol. 67, no. 15, pp. 3922–3937, Aug. 2019.
- [14] Z. Yu, Z. Liu, F. Meyer, A. Conti, and M. Z. Win, "Localization based on channel impulse response estimates," in *Proc. IEEE/ION PLANS-20*, 2020, pp. 1014–1021.
- [15] A. Richter, "Estimation of Radio Channel Parameters: Models and Algorithms," Ph.D. dissertation, Ilmenau University of Technology, 2005.
- [16] M. A. Badiu, T. L. Hansen, and B. H. Fleury, "Variational Bayesian inference of line spectra," *IEEE Trans. Signal Process.*, vol. 65, no. 9, pp. 2247–2261, May 2017.
- [17] M. S. Arulampalam, S. Maskell, N. Gordon, and T. Clapp, "A tutorial on particle filters for online nonlinear/non-Gaussian Bayesian tracking," *IEEE Trans. Signal Process.*, vol. 50, no. 2, pp. 174–188, Feb. 2002.
- [18] J. Karedal, S. Wyne, P. Almers, F. Tufvesson, and A. Molisch, "A measurement-based statistical model for industrial ultra-wideband channels," *IEEE Trans. Wireless Commun.*, vol. 6, no. 8, pp. 3028–3037, Aug. 2007.
- [19] A. Venus, E. Leitinger, S. Tertinek, and K. Witrisal, "Reliability and threshold-region performance of TOA estimators in dense multipath channels," in *Proc. IEEE ICC-WS-20*, 2020, pp. 1–7.
- [20] S. Kay, *Fundamentals of Statistical Signal Processing: Estimation Theory*. Upper Saddle River, NJ, USA: Prentice Hall, 1993.
- [21] —, *Fundamentals of Statistical Signal Processing: Detection Theory*. Upper Saddle River, NJ, USA: Prentice Hall, 1998.
- [22] E. Leitinger, S. Grebien, and K. Witrisal, "Multipath-based SLAM exploiting AoA and amplitude information," in *Proc. IEEE ICCW-19*, Shanghai, China, May 2019, pp. 1–7.
- [23] G. Papa, P. Braca, S. Horn, S. Marano, V. Matta, and P. Willett, "Adaptive Bayesian tracking with unknown time-varying sensor network performance," in *Proc. IEEE ICASSP-15*, 2015, pp. 2534–2538.
- [24] F. Meyer, T. Kropfreiter, J. L. Williams, R. Lau, F. Hlawatsch, P. Braca, and M. Z. Win, "Message passing algorithms for scalable multitarget tracking," *Proc. IEEE*, vol. 106, no. 2, pp. 221–259, Feb. 2018.
- [25] F. Kschischang, B. Frey, and H.-A. Loeliger, "Factor graphs and the sum-product algorithm," *IEEE Trans. Inf. Theory*, vol. 47, no. 2, pp. 498–519, Feb. 2001.
- [26] E. Leitinger, F. Meyer, F. Tufvesson, and K. Witrisal, "Factor graph based simultaneous localization and mapping using multipath channel information," in *Proc. IEEE ICCW-17*, Paris, France, May 2017, pp. 652–658.
- [27] Y. Bar-Shalom, T. Kirubarajan, and X.-R. Li, *Estimation with Applications to Tracking and Navigation*. New York, NY, USA: John Wiley & Sons, Inc., 2002.
- [28] D. B. Jourdan, D. Dardari, and M. Z. Win, "Position error bound for UWB localization in dense cluttered environments," *IEEE Trans. Aerosp. Electron. Syst.*, vol. 44, no. 2, pp. 613–628, 2008.
- [29] F. Meyer and J. L. Williams, "Scalable detection and tracking of extended objects," in *Proc. IEEE ICASSP-20*, Barcelona, Spain, May 2020, pp. 8916–8920.